

Registration of Histopathology Images Using Structural Information From Fine Grained Feature Maps

Dwarikanath Mahapatra

Inception Institute of Artificial Intelligence, Abu Dhabi, UAE

Abstract. Registration is an important part of many clinical workflows and factually, including information of structures of interest improves registration performance. We propose a novel approach of combining segmentation information in a registration framework using self supervised segmentation feature maps extracted using a pre-trained segmentation network followed by clustering. Using self supervised feature maps enables us to use segmentation information despite the unavailability of manual segmentations. Experimental results show our approach effectively replaces manual segmentation maps and demonstrate the possibility of obtaining state of the art registration performance in real world cases where manual segmentation maps are unavailable.

Keywords: Fine grained segmentation · Registration · Histopathology.

1 Introduction

An important part of a digital pathology image analysis workflow is the visual comparison of successive tissue sections enabling pathologists to evaluate histology and expression of multiple markers in a single area [25]. It has the potential to improve diagnostic accuracy and requires aligning all images to a common frame. Due to tissue processing and other procedures certain sections may undergo elastic deformations leading to shape changes across slices. Thus it is essential to have a reliable registration algorithm that can address challenges such as: (i) registration despite differences in tissue appearance (a consequence of different dyes and sample preparation); (ii) computing time due to large microscopy images; (iii) correcting complex elastic deformations, and (iv) difficulty of global unique features due to repetitive texture [1].

A comprehensive review on conventional image registration methods can be found in [107,13,70,16,12,10,48]. Although widely used, these methods are time consuming due to: 1) iterative optimization techniques; and 2) extensive parameter tuning. Deep learning (DL) methods can potentially overcome these limitations by using trained models to output registered images and deformation fields in much less time. In recent DL based image registration works, Sokooti et. al. [125,42,134,105,55,40] propose RegNet using CNNs trained on simulated deformations to register a pair of unimodal images. Vos et. al. [128,28,39,74,57,58]

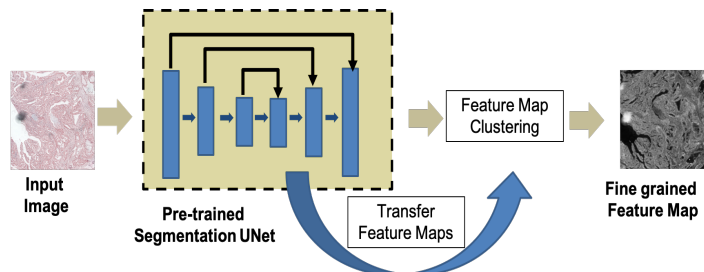
propose the deformable image registration network (DIRNet) which outputs a transformed image non-iteratively without having to train on known registration transformations. Rohe et. al. [112,75,78,36,35,38] propose SVF-Net that uses deformations obtained by registering previously segmented regions of interest (ROIs). The above methods are limited by the need of spatially corresponding patches ([125,128,34,99,97,95]) or being too dependent on training data. Balakrishnan et. al. [4,50,22,14,130,69] learn a parameterized registration function from a collection of training volumes, and in [3,52,72,119,120,45] they improve on their method by adding segmentation information.

Hu et al. in [19,121,51,115,114,126] propose a paradigm where registration is posed as a problem of segmenting corresponding regions of interest (ROIs) across images. Lee et al. in [27,123,82,122,81,133] register anatomical structures by mapping input images to spatial transformation parameters using Image-and-Spatial Transformer Networks (ISTNs). Liu et al. [29,54,53,59,79,104] propose feature-level probabilistic model to regularize CNN hidden layers for 3D brain image alignment. Hu et al. [18,24,77,118,76,86,117] use a two-stream 3D encoder-decoder network and pyramid registration module for registration.

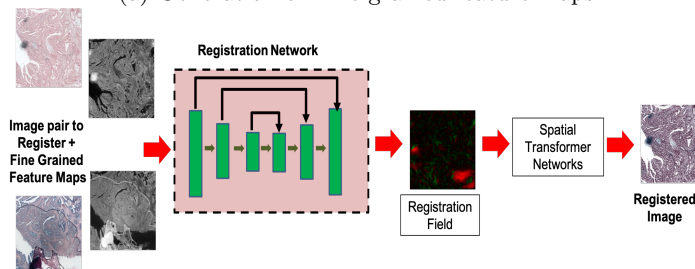
It is a well established fact that registration and segmentation are inter-related and mutually complementary. For example, labeled atlas images are used via image registration for segmentation while segmentation maps provide extra information to aid in image registration and result evaluation. Methods combining registration and segmentation have been proposed using active-contours [132,37,56,103,101,102,100], Bayesian methods [110,31,33,129,32,30,98] or Markov random field formulations [91,92,93,94,96,88,89]. Recent deep learning based approaches have used GANs [73,85,83,90,106,80] and a Deep Atlas [131,49,116,11,43,68,47] for joint registration and segmentation.

1.1 Contributions

While these methods show the advantages of integrating segmentation information with registration, they are dependent upon the availability of annotated segmentation maps during training. We propose a method to integrate structural information from self-supervised segmentation maps for registering histopathological images. Our approach does not require manual segmentation maps during training and test times. Self supervised approaches generate detailed segmentation feature maps of an image pair that provide fine grained information about the structures of interest. The structural information is included in the registration framework by means of a loss function that captures the structural similarity between the image pair being registered. Inclusion of the segmentation information contributes significantly to improved registration by providing the additional structural information that is so important for medical images. These maps are generated for the reference and floating image using a pre-trained semantic segmentation network and can be used for new images during test time.



(a) Generation of Fine grained feature maps



(b) Depiction of registration workflow

Fig. 1. Depiction of proposed workflow for generating fine grained feature maps and registration output.

2 Method

Figure 1 shows the workflow of our proposed approach. The reference image (I_R) and floating image (I_F) are passed through the pre-trained segmentation network to generate segmentation maps I_R^M and I_F^M . The maps and original images are input to a UNet architecture based network that outputs a registration field used by a spatial transformer network (STN) to output the transformed image.

2.1 Self Supervised Segmentation Feature Maps

Self-supervised learning is a variant of unsupervised learning methods, where a model learns to predict a set of labels that can be automatically created from the input data. A general approach is to train a CNN to perform an auxiliary task such as visual localization [26,23,17,87,46,41,44], predicting missing image parts [109,7,60,61,65,6,64], and cardiac MR image segmentation [2,5,66,67,63]. Defining an auxiliary task is dataset dependent and the same task/model may not be applicable when we aim to generalize the model to new dataset. Different from previous methods we generate self supervised segmentation maps by first extracting feature maps from a pre-trained segmentation network and then apply k-means clustering to generate a very detailed fine grained feature map.

We use a Fine-Grained Segmentation Network (FGSN) with a backbone UNet [113,62,84,71,111,8], that has been pre-trained on the Glas dataset [124]

for segmenting histopathological images. The architecture, shown in Figure 1 (a) has 3 convolution blocks each in the contracting (Encoder) and expanding (Decoder) path (shown as blue blocks). Each convolution block has 3 convolution layers of 3×3 filters, with ReLU activation and batch normalization. Each block is followed by 2×2 max pooling. Given the images I_R, I_F , we generate segmentation maps I_R^M, I_F^M . First we concatenate the maps of corresponding layers of the encoder and decoder part, upsample and fuse them to get feature maps. This allows us to integrate information from multiple scales.

After obtaining the feature maps we apply k -means clustering and the cluster assignments are used as labels. We can change the number of classes that the FGSN outputs without having to create new annotations. Higher the value of k denser are the segmentation maps. The initial feature maps are first clustered with a high value of $k = \frac{3N}{4}$ where N is the number of pixels, and reduce it as $k_{t+1} = 0.9k_t$, t being the iteration index. The optimum cluster number is determined using the Gap statistic method of [127] having the following steps:

1. Cluster the observed data by varying the number of clusters k and compute the corresponding total within intra-cluster variation W_k .
2. Generate B reference data sets with a random uniform distribution. Cluster each of these reference data sets with varying number of clusters, and compute the corresponding total within intra-cluster variation W_{kb} .
3. Compute the estimated gap statistic as the deviation of the observed W_k value from its expected value W_{kb} under the null hypothesis: $Gap(k) = \frac{1}{B} \sum_{b=1}^B \log(W_{kb}^*) - \log(W_k)$. Also compute the standard deviation.
4. Choose the number of clusters as the smallest value of k such that the gap statistic is within one standard deviation of the gap at $k+1$, i.e., $Gap(k) \geq Gap(k+1) - s_{k+1}$.

2.2 Registration using Segmentation Maps

Our primary contribution is the integration of segmentation features, generated in a self-supervised manner, into a deep learning based registration framework. Hence our approach is framework agnostic and can be used with various architectures. However, we choose to demonstrate our method’s effectiveness using the VoxelMorph architecture [3] because of two reasons: 1) In [3] the authors apply it for brain atlas registration on public datasets having manual segmentation maps. As a result they use a dice loss between manual segmentation maps in their training loss function. We aim to investigate if we can effectively replace the manual maps with our self supervised segmentation maps for the same image dataset. 2) secondly, since VoxelMorph has proven to be a popular baseline method for many works we investigate the improvements brought about by adding an additional segmentation loss from self supervised segmentation maps.

Figure 1 (b) shows the registration network architecture. Given reference and floating images I_R, I_F , we assume they have been affinely aligned, and only non-linear displacements exist between them. A Encoder-Decoder architecture is used for computing the deformation field φ which is used to transform I_F and

obtain the registered image $I_{Reg} = \varphi \circ I_F$ through spatial transformer networks (STNs) [20]. In an ideal registration I_R and I_{Reg} should match. Similar to the UNet architecture each block represents set of 3 2D convolution layers of kernel size 3, stride 2, followed by a LeakyReLU layer with parameter 0.2. The optimal parameter values are learned by minimizing differences between I_{Reg} and I_R . In order to use standard gradient-based methods, we construct a differentiable operation based on STN [20]

Loss Functions: We use two loss functions: an unsupervised loss L_{us} and an auxiliary loss L_a that leverages anatomical segmentations at training time. The unsupervised loss consists of two components: L_{sim} that penalizes differences in appearance, and L_{smooth} that penalizes local spatial variations in φ :

$$L_{us}(I_R, I_F, \varphi) = L_{sim}(I_R, I_{Reg}) + \lambda_1 L_{smooth}(\varphi) + \lambda_2 L_{seg}(M_R, M_F, M_{Reg}), \quad (1)$$

where $\lambda_1 = 0.95$, $\lambda_2 = 1.05$ are regularization parameters. L_{sim} is a combination of mean squared pixel intensity difference, and local cross correlation between I_R, I_{Reg} . L_{seg} is the segmentation loss function and is defined as

$$L_{seg}(M_R, M_{Reg}) = MSE(M_R, M_{Reg}) \quad (2)$$

which is the pixel wise difference between the segmentation maps of the reference and registered image. $M_{Reg} = \varphi \circ M_F$ is obtained by applying the deformation field φ to the segmentation map of the floating image being registered. A smooth displacement field φ is obtained using a diffusion regularizer on the spatial gradients of displacement u :

$$L_{smooth}(\varphi) = \sum_{p \in \Omega} \|\nabla u(p)\|^2 \quad (3)$$

3 Experimental Results

3.1 Implementation and Dataset Details

Our method was implemented in TensorFlow. We use Adam [21] with $\beta_1 = 0.93$ and batch normalization. The network was trained with 10^5 update iterations at learning rate 10^{-3} . Training and test was performed on a NVIDIA Titan X GPU with 12 GB RAM. We test our method on two datasets: 1) the publicly available ANHIR challenge dataset [1] used to evaluate automatic nonlinear image registration of 2D microscopy images of histopathology tissue samples stained with different dyes; and 2) a subset of the brain images used in [3]. Their descriptions are given below.

ANHIR Dataset: The dataset consists of 481 image pairs and is split into 230 training and 251 evaluation pairs [1]. For the training image pairs, both source and target landmarks are available, while for evaluation image pairs only source landmarks are available. The landmarks were annotated by 9 experts and

there are on an average 86 landmarks per image. The average error between the same landmarks chosen by two annotators is 0.05% of the image size which can be used as the indicator of the best possible results to achieve by the registration methods, below which the results become indistinguishable [9].

The images are divided into 8 classes containing: (i) lesion tissue, (ii) lung lobes, (iii) mammary glands, (iv) the colon adenocarcinomas, (v) mice kidney tissues, (vi) gastric mucosa and adenocarcinomas tissues, (vii) breast tissues, (viii) human kidney tissues. All the tissues were acquired in different acquisition settings making the dataset more diverse. The challenge was performed on medium size images which were approximately 25% of the original image scale. The approximate image size after the resampling varied from 8k to 16k pixels (in one dimension).

Brain Image Dataset: We used the 800 images of the ADNI-1 dataset [108] consisting of 200 controls, 400 MCI and 200 Alzheimer’s Disease patients. The MRI protocol for ADNI1 focused on consistent longitudinal structural imaging on 1.5T scanners using T1 and dual echo T2-weighted sequences. All scans were resampled to $256 \times 256 \times 256$ with 1mm isotropic voxels. Pre-processing includes affine registration and brain extraction using FreeSurfer [15], and cropping the resulting images to $160 \times 192 \times 224$. The dataset is split into 560, 120, and 120 volumes for training, validation, and testing. We simulate elastic deformations to generate the floating images using which we evaluate registration performance. Registration performance was calculated for 2D slices.

3.2 ANHIR Registration Results

Registration performance is evaluated using a normalized version of target registration error (TRE) and is defined as:

$$rTRE = \frac{TRE}{\sqrt{w^2 + h^2}} \quad (4)$$

where TRE is the target registration calculated as the Euclidean distance between corresponding landmarks in the two images and w, h are the image height and width respectively.

Table 1 summarizes the performance of $SR-Net$ (our proposed Segmentation based Registration NETWORK) and the top 2 methods on different tissue types. The median rTRE for all tissues and each individual tissue type is reported with the numbers taken from [1].

We perform a set of ablation experiments where we exclude the segmentation loss of Eqn.2 (denoted as $SR-Net_{wL_{seg}}$), using either MSE or cross correlation in L_{sim} of Eqn.1 (denoted, respectively, $SR-Net_{MSE}$, $SR-Net_{MSE}$). Since our registration framework is similar to VoxelMorph, $SR-Net_{wL_{seg}}$ is equivalent to VoxelMorph without the segmentation loss. The results show that SR-Net outperforms the top ranked methods for the challenge. Moreover, the advantages of using segmentation is also obvious by the fact that the rTRE values for $SR-Net_{wL_{seg}}$ are significantly higher than SR-Net ($p = 0.003$ from a paired Wilcoxon

	$SR - Net$	Rank 1	Rank 2	$SR-Net_{wSeg}$	$SR-Net_{MSE}$	$SR-Net_{CC}$
All	0.00099	0.00106	0.00183	0.00202	0.00196	0.00193
COADs	0.00123	0.00155	0.00198	0.00231	0.00214	0.00217
Breast tissue	0.00198	0.00222	0.00248	0.00293	0.00259	0.00263
human kidney	0.00231	0.00252	0.00259	0.00284	0.00273	0.00274
Gastric	0.00091	0.00122	0.00061	.00154	0.00139	0.00137
Lung lobes	0.00011	0.00008	0.00138	0.00167	0.00151	0.00157
Lung lesion	0.00010	0.00012	0.00534	.00591	0.00552	0.00567
Mice kidneys	0.00098	0.00104	0.00137	0.00171	0.00152	0.00160
Mammary gland	0.00017	0.00011	0.00266	0.00281	0.00273	0.00269

Table 1. Registration errors for different methods on the ANHIR dataset including ablation experiments. Values for *Rank 1*, *Rank 2* are taken from [1]

test). Ablation experiments also quantify the contribution of MSE and CC in the registration framework.

Figure 2 shows the registration results for pathology images where we show the reference and floating images alongwith the misalignment images before registration and after registration using SR-Net and $SR-Net_{wLSeg}$. The misalignment is greatly reduced after registration using SR-Net while in the case of $SR-Net_{wLSeg}$ there is still some resulting misalignment. This error can have significant consequences in the final diagnosis workflow. Hence the advantages of self-supervised segmentation maps are quite clear.

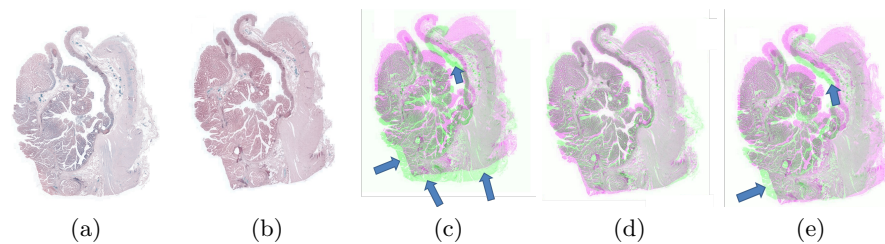


Fig. 2. Pathology image registration result: (a) I_R ; (b) I_F ; Misalignment of images: (c) before registration; after registration using (d) SR-Net; (e) $SR-Net_{wLSeg}$

3.3 Brain Image Registration

We apply $SR - Net$ to the brain image dataset. $SR - Net$'s difference w.r.t VoxelMorph is the use of self-supervised segmentation maps instead of manually annotated maps. The result is summarized in Table 2. SR-Net comes close to Voxel Morph's performance and there is no statistically significant difference between the results ($p = 0.031$). The numbers clearly show the significant improvement brought about by self supervised segmentation maps, to the extent

	Before	After Registration				
	Registration	SR-Net	SR-Net _{wL_{Seg}}	DIRNet	FlowNet	VoxelMorph
DM(%)	67.2	79.2	72.6	73.0	72.8	79.5
HD ₉₅ (mm)	14.5	12.1	13.7	13.4	13.5	11.9
Time(s)		0.5	0.4	0.6	0.5	0.5

Table 2. Registration results for different methods on brain images.

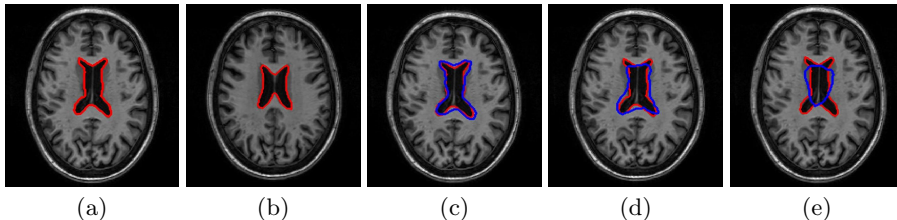


Fig. 3. Results for atlas based brain MRI image registration. (a) I_R (b) I_F with manual segmentation in red. Superimposed registered mask (in blue) obtained using: (c) SR-Net; (d) VoxelMorph; (e) SR-Net_{wL_{Seg}}.

that it performs at par when manual segmentation maps are used. VoxelMorph results can be considered the best possible performance under the given conditions and we are able to reach that with no manual segmentation maps.

Figure 3 shows results for brain image registration. We show the reference image in Figure 3 (a) followed by an example floating image in Figure 3 (b). The ventricle structure to be aligned is shown in red in both images. Figure 3 (c)-(e) shows the deformed structures obtained by applying the registration field obtained from different methods to the floating image and superimposing these structures on the atlas image. The deformed structures from the floating image are shown in blue. In case of perfect registration the blue and red contours should coincide. In this case SR-Net actually does better than VoxelMorph, while SR-Net_{wL_{Seg}} does significantly worse due to absence of segmentation information.

4 Conclusion

In this work we have proposed a deep learning based registration method that uses self supervised feature maps to include segmentation information in the registration framework. Use of self supervised segmentation maps enables us to include important structural information in scenarios where manual segmentation maps are unavailable, which is the case for majority of datasets. Experimental results show that by using self supervised segmentation maps the registration results are close to that obtained using manual segmentation maps. Hence we conclude that self supervised segmentation maps are an effective way of replacing manual segmentation maps and obtaining improved registration. This is applicable for majority of medical image analysis tasks where registration is essential and manual segmentation maps are unavailable.

References

1. ANHIR: Automatic non-rigid histological image registration challenge. <https://anhir.grand-challenge.org/>, accessed: 2020-01-30
2. Bai, W., Chen, C., Tarroni, G., Duan, J., Guitton, F., Petersen, S.E., Guo, Y., Matthews, P.M., Rueckert, D.: Self-supervised learning for cardiac mr image segmentation by anatomical position prediction. In: In Proc. MICCAI. pp. 234–241 (2019)
3. Balakrishnan, G., Zhao, A., Sabuncu, M.R., Guttag, J., Dalca, A.V.: Voxelmorph: a learning framework for deformable medical image registration. *IEEE Trans. Med. Imag.* **38**(8), 1788–1800 (2019)
4. Balakrishnan, G., Zhao, A., Sabuncu, M., Guttag, J.: An supervised learning model for deformable medical image registration. In: Proc. CVPR. pp. 9252–9260 (2018)
5. Bastide, P., Kiral-Kornek, I., Mahapatra, D., Saha, S., Vishwanath, A., Cavallar, S.V.: Machine learned optimizing of health activity for participants during meeting times. In: US Patent App. 15/426,634 (2018)
6. Bastide, P., Kiral-Kornek, I., Mahapatra, D., Saha, S., Vishwanath, A., Cavallar, S.V.: Visual health maintenance and improvement. In: US Patent 9,993,385 (2018)
7. Bastide, P., Kiral-Kornek, I., Mahapatra, D., Saha, S., Vishwanath, A., Cavallar, S.V.: Crowdsourcing health improvements routes. In: US Patent App. 15/611,519 (2019)
8. BJ Antony, S Sedai, D.M.R.G.: Real-time passive monitoring and assessment of pediatric eye health. In: US Patent App. US Patent App. 16/178,757 (2020)
9. Borovec, J., Munoz-Barrutia, A., Kybic, J.: Benchmarking of image registration methods for differently stained histological slides. In: In Proc. IEEE ICIP. pp. 3368–3372 (2018)
10. Bozorgtabar, B., Mahapatra, D., von Teng, H., Pollinger, A., Ebner, L., Thiran, J.P., Reyes, M.: Informative sample generation using class aware generative adversarial networks for classification of chest xrays. *Computer Vision and Image Understanding* **184**, 57–65 (2019)
11. Bozorgtabar, B., Mahapatra, D., von Teng, H., Pollinger, A., Ebner, L., Thiran, J.P., Reyes, M.: Informative sample generation using class aware generative adversarial networks for classification of chest xrays. In: arXiv preprint arXiv:1904.10781 (2019)
12. Bozorgtabar, B., Mahapatra, D., Thiran, J.P.: Exprada: Adversarial domain adaptation for facial expression analysis. In *Press Pattern Recognition* **100**, 15–28 (2020)
13. Bozorgtabar, B., Mahapatra, D., Zlobec, I., Rau, T., Thiran, J.: Computational pathology. *Frontiers in Medicine* **7** (2020)
14. Bozorgtabar, B., Rad, M.S., Mahapatra, D., Thiran, J.P.: Syndemo: Synergistic deep feature alignment for joint learning of depth and ego-motion. In: In Proc. IEEE ICCV (2019)
15. Fischl, B.: Freesurfer. *Neuroimage* **62**(2), 774–781 (2015)
16. Ge, Z., Mahapatra, D., Chang, X., Chen, Z., Chi, L., Lu, H.: Improving multi-label chest x-ray disease diagnosis by exploiting disease and health labels dependencies. In *press Multimedia Tools and Application* **1**, 1–14 (2019)
17. Ge, Z., Mahapatra, D., Sedai, S., Garnavi, R., Chakravorty, R.: Chest x-rays classification: A multi-label and fine-grained problem. In: arXiv preprint arXiv:1807.07247 (2018)

18. Hu, X., Kang, M., Huang, W., Scott, M.R., Wiest, R., Reyes, M.: Dual-stream pyramid registration network. In: Proc. MICCAI. pp. 382–390 (2019)
19. Hu, Y., Gibson, E., Barratt, D.C., Emberton, M., Noble, J.A., Vercauteren, T.: Conditional segmentation in lieu of image registration. In: Proc. MICCAI. pp. 401–409 (2019)
20. Jaderberg, M., Simonyan, K., Zisserman, A., Kavukcuoglu, K.: Spatial transformer networks. In: NIPS. pp. – (2015)
21. Kingma, D., Ba, J.: Adam: A method for stochastic optimization. In: International Conference on Learning Representations, (2014)
22. Kuanar, S., Athitsos, V., Mahapatra, D., Rao, K., Akhtar, Z., Dasgupta, D.: Low dose abdominal ct image reconstruction: An unsupervised learning based approach. In: In Proc. IEEE ICIP. pp. 1351–1355 (2019)
23. Kuanar, S., Rao, K., Mahapatra, D., Bilas, M.: Night time haze and glow removal using deep dilated convolutional network. In: arXiv preprint arXiv:1902.00855 (2019)
24. Kuang, H., Guthier, B., Saini, M., Mahapatra, D., Saddik, A.E.: A real-time smart assistant for video surveillance through handheld devices. In: In Proc: ACM Intl. Conf. Multimedia. pp. 917–920 (2014)
25. Kugler, M., , et al.: Robust 3d image reconstruction of pancreatic cancer tumors from histopathological images with different stains and its quantitative performance evaluation. Intl. J. Comp. Assisted Radiology and Surgery **14**, 2047–2055 (2019)
26. Larsson, M., Stenborg, E., Toft, C., Hammarstrand, L., Sattler, T., Kahl, F.: Fine-grained segmentation networks: Self-supervised segmentation for improved long-term visual localization. In: In Proc ICCV. pp. 31–41 (2019)
27. Lee, M., Oktay, O., Schuh, A., Schaap, M., Glocker, B.: Image-and-spatial transformer networks for structure-guided image registration. In: Proc. MICCAI. pp. 337–345 (2019)
28. Li, Z., Mahapatra, D., J.Tielbeek, Stoker, J., van Vliet, L., Vos, F.: Image registration based on autocorrelation of local structure. IEEE Trans. Med. Imaging **35**(1), 63–75 (2016)
29. Liu, L., Hu, X., Zhu, L., Heng, P.A.: Probabilistic multilayer regularization network for unsupervised 3d brain image registration. In: Proc. MICCAI. pp. 346–354 (2019)
30. Mahapatra, D.: Neonatal brain mri skull stripping using graph cuts and shape priors. In: In Proc: MICCAI workshop on Image Analysis of Human Brain Development (IAHBD) (2011)
31. Mahapatra, D.: Cardiac lv and rv segmentation using mutual context information. In: Proc. MICCAI-MLMI. pp. 201–209 (2012)
32. Mahapatra, D.: Groupwise registration of dynamic cardiac perfusion images using temporal information and segmentation information. In: In Proc: SPIE Medical Imaging (2012)
33. Mahapatra, D.: Landmark detection in cardiac mri using learned local image statistics. In: Proc. MICCAI-Statistical Atlases and Computational Models of the Heart. Imaging and Modelling Challenges (STACOM). pp. 115–124 (2012)
34. Mahapatra, D.: Skull stripping of neonatal brain mri: Using prior shape information with graphcuts. J. Digit. Imaging **25**(6), 802–814 (2012)
35. Mahapatra, D.: Cardiac image segmentation from cine cardiac mri using graph cuts and shape priors. J. Digit. Imaging **26**(4), 721–730 (2013)
36. Mahapatra, D.: Cardiac mri segmentation using mutual context information from left and right ventricle. J. Digit. Imaging **26**(5), 898–908 (2013)

37. Mahapatra, D.: Graph cut based automatic prostate segmentation using learned semantic information. In: Proc. IEEE ISBI. pp. 1304–1307 (2013)
38. Mahapatra, D.: Joint segmentation and groupwise registration of cardiac perfusion images using temporal information. *J. Digit. Imaging* **26**(2), 173–182 (2013)
39. Mahapatra, D.: Automatic cardiac segmentation using semantic information from random forests. *J. Digit. Imaging*. **27**(6), 794–804 (2014)
40. Mahapatra, D.: Combining multiple expert annotations using semi-supervised learning and graph cuts for medical image segmentation. *Computer Vision and Image Understanding* **151**(1), 114–123 (2016)
41. Mahapatra, D.: Consensus based medical image segmentation using semi-supervised learning and graph cuts. In: arXiv preprint arXiv:1612.02166 (2017)
42. Mahapatra, D.: Semi-supervised learning and graph cuts for consensus based medical image segmentation. *Pattern Recognition* **63**(1), 700–709 (2017)
43. Mahapatra, D.: Amd severity prediction and explainability using image registration and deep embedded clustering. In: arXiv preprint arXiv:1907.03075 (2019)
44. Mahapatra, D., Agarwal, K., Khosrowabadi, R., Prasad, D.: Recent advances in statistical data and signal analysis: Application to real world diagnostics from medical and biological signals. In: *Computational and mathematical methods in medicine* (2016)
45. Mahapatra, D., Antony, B., Sedai, S., Garnavi, R.: Deformable medical image registration using generative adversarial networks. In: In Proc. IEEE ISBI. pp. 1449–1453 (2018)
46. Mahapatra, D., Bozorgtabar, B.: Retinal vasculature segmentation using local saliency maps and generative adversarial networks for image super resolution. In: arXiv preprint arXiv:1710.04783 (2017)
47. Mahapatra, D., Bozorgtabar, B.: Progressive generative adversarial networks for medical image super resolution. In: arXiv preprint arXiv:1902.02144 (2019)
48. Mahapatra, D., Bozorgtabar, B., Garnavi, R.: Image super-resolution using progressive generative adversarial networks for medical image analysis. *Computerized Medical Imaging and Graphics* **71**, 30–39 (2019)
49. Mahapatra, D., Bozorgtabar, B., Shao, J.P.T.L.: Pathological retinal region segmentation from oct images using geometric relation based augmentation (2020)
50. Mahapatra, D., Bozorgtabar, B., Shao, L.: Pathological retinal region segmentation from oct images using geometric relation based augmentation. In: In Proc. IEEE CVPR. pp. 9611–9620 (2020)
51. Mahapatra, D., Bozorgtabar, S., Hewavitahranage, S., Garnavi, R.: Image super resolution using generative adversarial networks and local saliency maps for retinal image analysis,. In: In Proc. MICCAI. pp. 382–390 (2017)
52. Mahapatra, D., Bozorgtabar, S., Thiran, J.P., Reyes, M.: Efficient active learning for image classification and segmentation using a sample selection and conditional generative adversarial network. In: In Proc. MICCAI (2). pp. 580–588 (2018)
53. Mahapatra, D., Buhmann, J.: Obtaining consensus annotations for retinal image segmentation using random forest and graph cuts. In: In Proc. OMIA. pp. 41–48 (2015)
54. Mahapatra, D., Buhmann, J.: Visual saliency based active learning for prostate mri segmentation. In: In Proc. MLMI. pp. 9–16 (2015)
55. Mahapatra, D., Buhmann, J.: Visual saliency based active learning for prostate mri segmentation. *SPIE Journal of Medical Imaging* **3**(1) (2016)
56. Mahapatra, D., Buhmann, J.: Automatic cardiac rv segmentation using semantic information with graph cuts. In: Proc. IEEE ISBI. pp. 1094–1097 (2013)

57. Mahapatra, D., Buhmann, J.: Analyzing training information from random forests for improved image segmentation. *IEEE Trans. Imag. Proc.* **23**(4), 1504–1512 (2014)
58. Mahapatra, D., Buhmann, J.: Prostate mri segmentation using learned semantic knowledge and graph cuts. *IEEE Trans. Biomed. Engg.* **61**(3), 756–764 (2014)
59. Mahapatra, D., Buhmann, J.: A field of experts model for optic cup and disc segmentation from retinal fundus images. In: *In Proc. IEEE ISBI*. pp. 218–221 (2015)
60. Mahapatra, D., Garnavi, R., Roy, P., Tennakoon, R.: System and method to teach and evaluate image grading performance using prior learned expert knowledge base. In: *US Patent App. 15/459,457* (2018)
61. Mahapatra, D., Garnavi, R., Roy, P., Tennakoon, R.: System and method to teach and evaluate image grading performance using prior learned expert knowledge base. In: *US Patent App. 15/814,590* (2018)
62. Mahapatra, D., Garnavi, R., Sedai, S., Roy, P.: Joint segmentation and characteristics estimation in medical images. In: *US Patent App. 15/234,426* (2017)
63. Mahapatra, D., Garnavi, R., Sedai, S., Roy, P.: Retinal image quality assessment, error identification and automatic quality correction. In: *US Patent 9,779,492* (2017)
64. Mahapatra, D., Garnavi, R., Sedai, S., Tennakoon, R.: Classification of severity of pathological condition using hybrid image representation. In: *US Patent App. 15/426,634* (2018)
65. Mahapatra, D., Garnavi, R., Sedai, S., Tennakoon, R.: Generating an enriched knowledge base from annotated images. In: *US Patent App. 15/429,735* (2018)
66. Mahapatra, D., Garnavi, R., Sedai, S., Tennakoon, R., Chakravorty, R.: Early prediction of age related macular degeneration by image reconstruction. In: *US Patent App. 15/854,984* (2018)
67. Mahapatra, D., Garnavi, R., Sedai, S., Tennakoon, R., Chakravorty, R.: Early prediction of age related macular degeneration by image reconstruction. In: *US Patent 9,943,225* (2018)
68. Mahapatra, D., Ge, Z.: Combining transfer learning and segmentation information with gans for training data independent image registration. In: *arXiv preprint arXiv:1903.10139* (2019)
69. Mahapatra, D., Ge, Z.: Training data independent image registration with gans using transfer learning and segmentation information. In: *In Proc. IEEE ISBI*. pp. 709–713 (2019)
70. Mahapatra, D., Ge, Z.: Training data independent image registration using generative adversarial networks and domain adaptation. *Pattern Recognition* **100**, 1–14 (2020)
71. Mahapatra, D., Ge, Z., Sedai, S.: Joint registration and segmentation of images using deep learning. In: *US Patent App. 16/001,566* (2019)
72. Mahapatra, D., Ge, Z., Sedai, S., Chakravorty, R.: Joint registration and segmentation of xray images using generative adversarial networks. In: *In Proc. MICCAI-MLMI*. pp. 73–80 (2018)
73. Mahapatra, D., Ge, Z., Sedai, S., Chakravorty, R.: Joint registration and segmentation of xray images using generative adversarial networks. In: *MICCAI-MLMI*. pp. 73–80 (2018)
74. Mahapatra, D., Gilani, S., Saini, M.: Coherency based spatio-temporal saliency detection for video object segmentation. *IEEE Journal of Selected Topics in Signal Processing.* **8**(3), 454–462 (2014)

75. Mahapatra, D., J.Tielbeek, Makanyanga, J., Stoker, J., Taylor, S., Vos, F., Buhmann, J.: Automatic detection and segmentation of crohn's disease tissues from abdominal mri. *IEEE Trans. Med. Imaging* **32**(12), 1232–1248 (2013)
76. Mahapatra, D., J.Tielbeek, Makanyanga, J., Stoker, J., Taylor, S., Vos, F., Buhmann, J.: Active learning based segmentation of crohn's disease using principles of visual saliency. In: *Proc. IEEE ISBI*. pp. 226–229 (2014)
77. Mahapatra, D., J.Tielbeek, Makanyanga, J., Stoker, J., Taylor, S., Vos, F., Buhmann, J.: Combining multiple expert annotations using semi-supervised learning and graph cuts for crohn's disease segmentation. In: *In Proc: MICCAI-ABD* (2014)
78. Mahapatra, D., J.Tielbeek, Vos, F., Buhmann, J.: A supervised learning approach for crohn's disease detection using higher order image statistics and a novel shape asymmetry measure. *J. Digit. Imaging* **26**(5), 920–931 (2013)
79. Mahapatra, D., Li, Z., Vos, F., Buhmann, J.: Joint segmentation and groupwise registration of cardiac dce mri using sparse data representations. In: *In Proc. IEEE ISBI*. pp. 1312–1315 (2015)
80. Mahapatra, D., Routray, A., Mishra, C.: An active snake model for classification of extreme emotions. In: *IEEE International Conference on Industrial Technology (ICIT)*. pp. 2195–2199 (2006)
81. Mahapatra, D., Roy, P., Sedai, S., Garnavi, R.: A cnn based neurobiology inspired approach for retinal image quality assessment. In: *In Proc. EMBC*. pp. 1304–1307 (2016)
82. Mahapatra, D., Roy, P., Sedai, S., Garnavi, R.: Retinal image quality classification using saliency maps and cnns. In: *In Proc. MICCAI-MLMI*. pp. 172–179 (2016)
83. Mahapatra, D., Roy, S., Sun, Y.: Retrieval of mr kidney images by incorporating spatial information in histogram of low level features. In: *In 13th International Conference on Biomedical Engineering* (2008)
84. Mahapatra, D., Saha, S., Vishwanath, A., Bastide, P.: Generating hyperspectral image database by machine learning and mapping of color images to hyperspectral domain. In: *US Patent App. 15/949,528* (2019)
85. Mahapatra, D., Saini, M., Sun, Y.: Illumination invariant tracking in office environments using neurobiology-saliency based particle filter. In: *IEEE ICME*. pp. 953–956 (2008)
86. Mahapatra, D., Schüffler, P., Tielbeek, J., Vos, F., Buhmann, J.: Semi-supervised and active learning for automatic segmentation of crohn's disease. In: *Proc. MICCAI, Part 2*. pp. 214–221 (2013)
87. Mahapatra, D., Sedai, S., Garnavi, R.: Elastic registration of medical images with gans. In: *arXiv preprint arXiv:1805.02369* (2018)
88. Mahapatra, D., Sun, Y.: Nonrigid registration of dynamic renal MR images using a saliency based MRF model. In: *Proc. MICCAI*. pp. 771–779 (2008)
89. Mahapatra, D., Sun, Y.: Registration of dynamic renal mr images using neurobiological model of saliency. In: *Proc. ISBI*. pp. 1119–1122 (2008)
90. Mahapatra, D., Sun, Y.: Using saliency features for graphcut segmentation of perfusion kidney images. In: *In 13th International Conference on Biomedical Engineering* (2008)
91. Mahapatra, D., Sun, Y.: Joint registration and segmentation of dynamic cardiac perfusion images using mrfs. In: *Proc. MICCAI*. pp. 493–501 (2010)
92. Mahapatra, D., Sun, Y.: Joint registration and segmentation of dynamic cardiac perfusion images using mrfs. In: *Proc. MICCAI*. pp. 493–501 (2010)
93. Mahapatra, D., Sun, Y.: An mrf framework for joint registration and segmentation of natural and perfusion images. In: *Proc. IEEE ICIP*. pp. 1709–1712 (2010)

94. Mahapatra, D., Sun, Y.: Retrieval of perfusion images using cosegmentation and shape context information. In: Proc. APSIPA Annual Summit and Conference (ASC) (2010)
95. Mahapatra, D., Sun, Y.: Rigid registration of renal perfusion images using a neurobiology based visual saliency model. EURASIP Journal on Image and Video Processing. pp. 1–16 (2010)
96. Mahapatra, D., Sun, Y.: A saliency based mrf method for the joint registration and segmentation of dynamic renal mr images. In: Proc. ICDIP (2010)
97. Mahapatra, D., Sun, Y.: Mrf based intensity invariant elastic registration of cardiac perfusion images using saliency information. IEEE Trans. Biomed. Engg. **58**(4), 991–1000 (2011)
98. Mahapatra, D., Sun, Y.: Orientation histograms as shape priors for left ventricle segmentation using graph cuts. In: In Proc: MICCAI. pp. 420–427 (2011)
99. Mahapatra, D., Sun, Y.: Integrating segmentation information for improved mrf-based elastic image registration. IEEE Trans. Imag. Proc. **21**(1), 170–183 (2012)
100. Mahapatra, D., Tielbeek, J., Buhmann, J., Vos, F.: A supervised learning based approach to detect crohn’s disease in abdominal mr volumes. In: Proc. MICCAI workshop Computational and Clinical Applications in Abdominal Imaging(MICCAI-ABD). pp. 97–106 (2012)
101. Mahapatra, D., Tielbeek, J., Vos, F., ., J.B.: Crohn’s disease tissue segmentation from abdominal mri using semantic information and graph cuts. In: Proc. IEEE ISBI. pp. 358–361 (2013)
102. Mahapatra, D., Tielbeek, J., Vos, F., Buhmann, J.: Localizing and segmenting crohn’s disease affected regions in abdominal mri using novel context features. In: Proc. SPIE Medical Imaging (2013)
103. Mahapatra, D., Tielbeek, J., Vos, F., Buhmann, J.: Weakly supervised semantic segmentation of crohn’s disease tissues from abdominal mri. In: Proc. IEEE ISBI. pp. 832–835 (2013)
104. Mahapatra, D., Vos, F., Buhmann, J.: Crohn’s disease segmentation from mri using learned image priors. In: In Proc. IEEE ISBI. pp. 625–628 (2015)
105. Mahapatra, D., Vos, F., Buhmann, J.: Active learning based segmentation of crohns disease from abdominal mri. Computer Methods and Programs in Biomedicine **128**(1), 75–85 (2016)
106. Mahapatra, D., Winkler, S., Yen, S.: Motion saliency outweighs other low-level features while watching videos. In: SPIE HVEI. pp. 1–10 (2008)
107. maintz, J., Viergever, M.: A survey of medical image registration. Med. Imag. Anal **2**(1), 1–36 (1998)
108. Mueller, S.G.: Ways toward an early diagnosis in alzheimers disease: the alzheimers disease neuroimaging initiative (ADNI). Alzheimers & Dementia **1**(1), 55–66 (2005)
109. Pathak, D., Krahenbuhl, P., Donahue, J., Darrell, T., Efros, A.A.: Context encoders: Feature learning by inpainting. In: In Proc CVPR. pp. 31–41 (2016)
110. Pohl, K.M., Fisher, J., Grimson, W.E.L., Kikinis, R., Wells, W.M.: A Bayesian model for joint segmentation and registration. NeuroImage **31**(1), 228–239 (2006)
111. R Garnavi, D Mahapatra, P.R.R.T.: System and method to teach and evaluate image grading performance using prior learned expert knowledge base. In: US Patent App. 10,657,838 (2020)
112. Rohe, M., Datar, M., Heimann, T., Sermesant, M., Pennec, X.: SVF-Net: Learning deformable image registration using shape matching. In: In Proc.MICCAI. pp. 266–274 (2017)

113. Ronneberger, O., Fischer, P., Brox, T.: U-net: Convolutional networks for biomedical image segmentation. In: In Proc. MICCAI. pp. 234–241 (2015)
114. Roy, P., Chakravorty, R., Sedai, S., Mahapatra, D., Garnavi, R.: Automatic eye type detection in retinal fundus image using fusion of transfer learning and anatomical features. In: In Proc. DICTA. pp. 1–7 (2016)
115. Roy, P., Tennakoon, R., Cao, K., Sedai, S., Mahapatra, D., Maetschke, S., Garnavi, R.: A novel hybrid approach for severity assessment of diabetic retinopathy in colour fundus images,. In: In Proc. IEEE ISBI. pp. 1078–1082 (2017)
116. Saini, M., Guthier, B., Kuang, H., Mahapatra, D., Saddik, A.: szoom: A framework for automatic zoom into high resolution surveillance videos. In: arXiv preprint arXiv:1909.10164 (2019)
117. Schüffler, P., Mahapatra, D., Tielbeek, J., Vos, F., Makanyanga, J., Pends, D., Nio, C., Stoker, J., Taylor, S., Buhmann, J.: A model development pipeline for crohns disease severity assessment from magnetic resonance images. In: In Proc: MICCAI-ABD (2013)
118. Schüffler, P., Mahapatra, D., Tielbeek, J., Vos, F., Makanyanga, J., Pends, D., Nio, C., Stoker, J., Taylor, S., Buhmann, J.: Semi automatic crohns disease severity assessment on mr imaging. In: In Proc: MICCAI-ABD (2014)
119. Sedai, S., Mahapatra, D., Antony, B., Garnavi, R.: Joint segmentation and uncertainty visualization of retinal layers in optical coherence tomography images using bayesian deep learning. In: In Proc. MICCAI-OMIA. pp. 219–227 (2018)
120. Sedai, S., Mahapatra, D., Ge, Z., Chakravorty, R., Garnavi, R.: Deep multiscale convolutional feature learning for weakly supervised localization of chest pathologies in x-ray images. In: In Proc. MICCAI-MLMI. pp. 267–275 (2018)
121. Sedai, S., Mahapatra, D., Hewavitharanage, S., Maetschke, S., Garnavi, R.: Semi-supervised segmentation of optic cup in retinal fundus images using variational autoencoder,. In: In Proc. MICCAI. pp. 75–82 (2017)
122. Sedai, S., Roy, P., Mahapatra, D., Garnavi, R.: Segmentation of optic disc and optic cup in retinal fundus images using shape regression. In: In Proc. EMBC. pp. 3260–3264 (2016)
123. Sedai, S., Roy, P., Mahapatra, D., Garnavi, R.: Segmentation of optic disc and optic cup in retinal images using coupled shape regression. In: In Proc. MICCAI-OMIA. pp. 1–8 (2016)
124. Sirinukunwattana, K., , et al.: Gland segmentation in colon histology images: The GlaS challenge contest. *Med. Imag. Anal.* **35**, 489–502 (2017)
125. Sokooti, H., de Vos, B., Berendsen, F., Lelieveldt, B., Isgum, I., Staring, M.: Nonrigid image registration using multiscale 3d convolutional neural networks. In: MICCAI. pp. 232–239 (2017)
126. Tennakoon, R., Mahapatra, D., Roy, P., Sedai, S., Garnavi, R.: Image quality classification for dr screening using convolutional neural networks. In: In Proc. MICCAI-OMIA. pp. 113–120 (2016)
127. Tibshirani, R., Walther, G., Hastie, T.: Estimating the number of clusters in a data set via the gap statistic. *J. R. Statistical Society (B)* **63**(2), 411423 (2001)
128. de Vos, B., Berendsen, F., Viergever, M., Staring, M., Isgum, I.: End-to-end unsupervised deformable image registration with a convolutional neural network. In: MICCAI International Workshop on Deep Learning in Medical Image Analysis. pp. 204–212 (2017)
129. Vos, F.M., Tielbeek, J., Naziroglu, R., Li, Z., Schüffler, P., Mahapatra, D., Wiebel, A., Lavini, C., Buhmann, J., Hege, H., Stoker, J., van Vliet, L.: Computational modeling for assessment of IBD: to be or not to be? In: Proc. IEEE EMBC. pp. 3974–3977 (2012)

130. Xing, Y., Ge, Z., Zeng, R., Mahapatra, D., Seah, J., Law, M., Drummond, T.: Adversarial pulmonary pathology translation for pairwise chest x-ray data augmentation. In: In Proc. MICCAI. pp. 757–765 (2019)
131. Xu, Z., Niethammer, M.: DeepAtlas: Joint semi-supervised learning of image registration and segmentation. In: Proc. MICCAI. pp. 420–429 (2019)
132. Yezzi, A., Zollei, L., Kapur, T.: A variational framework for joint segmentation and registration. In: Proc. MMBIA. pp. 44–51 (2001)
133. Zilly, J., Buhmann, J., Mahapatra, D.: Boosting convolutional filters with entropy sampling for optic cup and disc image segmentation from fundus images. In: In Proc. MLMI. pp. 136–143 (2015)
134. Zilly, J., Buhmann, J., Mahapatra, D.: Glaucoma detection using entropy sampling and ensemble learning for automatic optic cup and disc segmentation. In Press *Computerized Medical Imaging and Graphics* **55**(1), 28–41 (2017)